Simple 60 GHz Switched Beam Antenna for 5G Millimeter-Wave Applications

Kamil Trzebiatowski, Mateusz Rzymowski, *Member, IEEE*, Lukasz Kulas, *Senior Member, IEEE*, and Krzysztof Nyka, *Senior Member, IEEE*

***Abstract*—A new 60 GHz band single-input switched beam antenna is proposed for the fifth-generation (5G) millimeter-wave network applications. The presented design is capable of electronically switching the main beam in two different directions via a proposed microstrip-line-to-slotline single-pole dual-throw (SPDT) switch based on commercially available p-i-n diodes. The antenna is fabricated in a low-cost printed circuit board process on a CuClad 217 substrate. Measurements were carried out in an anechoic chamber and experimental results show good agreement with numerical simulations. The antenna is capable of switching the main beam to the $+45°$ and $-45°$ directions in the horizontal plane with a gain of about 3 dBi and a beamwidth of 80° in both states. The presented prototype shows several advantages over other state-of-the-art millimeter-wave reconfigurable antennas such as a simple electrical switching mechanism, low-cost manufacturing, a low profile, and a small footprint. These features make the presented antenna ideal for low-cost millimeter-wave 5G applications, particularly in end-devices working under the Internet-of-Things paradigm.**

***Index Terms*—Fifth generation (5G), Internet-of-Things, millimeter-wave antenna, p-i-n diode, reconfigurable antennas, single-pole dual-throw (SPDT) switch, slot antennas, switched-beam antennas.**

I. Introduction

IN MODERN fifth-generation (5G) communication systems there is an increasing demand for exchanging huge amount of data from end-devices with small latency, as well as expectations that the devices will have reduced size and improved energy efficiency. A millimeter wave technology seems to address these emerging needs [1], [2]. The 60 GHz ISM band available for nonlicensed operation is considered for complementary solutions of reliable and wideband 5G communication inside the buildings [3]. The main issues that should be considered with respect to this technology are limited operation range, sensitivity to changing propagation environment and coexistence with other ISM wireless systems that may affect the communication quality. The first two limitations are caused by the propagation properties of the millimeter waves and have to be handled especially with regard to dynamically changing and harsh industrial environments.

Antenna arrays are often used to overcome the propagation issues as by increasing the number of antenna elements it is possible to generate a narrow directional beam with high gain [4] which, however, significantly limits the angular coverage of communication. This can be solved by antennas with steerable beam where a set of directional radiation patterns is available to increase coverage of the system. There is a number of potential solutions that allow for precise beam steering but they are complicated due to complex switching circuits [5], [6], or advanced signal processing in case of digital beamforming [6]. Interesting candidates that can be considered for low-cost applications are switched beam antennas [5], which have already been proven in lower frequency bands to improve wireless network connectivity [7]–[10].

Various designs of switched beam antennas for the millimeter-wave bands have been proposed in [5] and [11]–[18]. The concepts of integrating beamforming feed networks, such as Butler matrices or Rotman lenses, with the RF switching circuits have been presented in [11]–[13]. A four-element antenna with FET switch ICs and a dielectric lens has been proposed in [14]. Another approach is to use transmitarrays [15] with the antenna elements placed on the back focal plane of the focusing element [5]. The main drawbacks of the above designs are large size and high losses which deteriorate the antenna gain. The solutions based on switched elements radiating in different directions were investigated in [16]–[18]. However, these designs can be difficult to manufacture due to the strict technological requirements.

An interesting switched beam antenna was demonstrated in [19], where four linear tapered slot antennas (LTSA) are switched by changing the state of p-i-n diodes placed in the feeding slots. The antenna has one dielectric layer and is manufactured in a printed circuit board (PCB) process but is proposed only for the 2.4 GHz frequency range. The design is relatively small compared to the wavelength and is an interesting inspiration for implementing a similar concept in millimeter-wave frequencies.

This letter presents the design of a novel simple 60 GHz switched beam antenna fabricated in a standard low-cost PCB

Manuscript received October 7, 2020; revised October 26, 2020; accepted November 11, 2020. Date of publication November 16, 2020; date of current version January 14, 2021. This work was supported in part by SCOTT under Grant 737422, and in part by AFARCLOUD under Grant 783221, projects that have received funding from the Electronic Component Systems for European Leadership Joint Undertaking. This Joint Undertaking receives support from the European Union's Horizon 2020 Research and Innovation Programme, and Austria, Belgium, Czech Republic, Finland, Germany, Greece, Ireland, Italy, Latvia, The Netherlands, Norway, Poland, Portugal, Spain, Sweden. *(Corresponding author: Kamil Trzebiatowski.)*

The authors are with the Department of Microwave and Antenna Engineering, Faculty of Electronics, Telecommunications, and Informatics, Gdansk University of Technology, 80-233 Gdansk, Poland (e-mail: kamil.trzebiatowski@pg.edu.pl; mateusz.rzymowski@pg.edu.pl; lukasz.kulas@eti.pg.gda.pl; krzysztof.nyka@pg.edu.pl).

Digital Object Identifier 10.1109/LAWP.2020.3038260

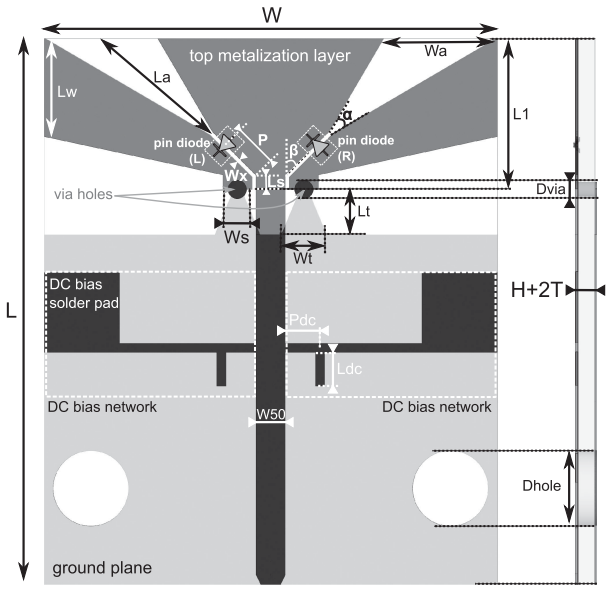

Fig. 1. Design of the proposed antenna (a top-down view). The top layer metallization is in black and dark gray, while the ground plane is in light gray. See Table I for dimension values.

TABLE I
DESIGN DIMENSIONS OF THE ANTENNA, ALL DIMENSIONS IN mm EXCEPT ANGLES THAT ARE IN DEGREES

L	W	L_a	W_a	W_s	W_x	W_{50}	W_t	L_t
14.7	11.9	3.83	2.96	0.78	0.15	0.78	1.2	1.2
P	L_1	L_w	L_s	L_{dc}	P_{dc}	D_{via}	α	β
1.2	4.0	2.6	0.33	0.89	0.92	0.4	30	45

technology and is dedicated to the future industrial end-devices operating in harsh propagation environments. Proposed antenna can change its main lobe direction between two different angles using commercially available p-i-n diodes. In comparison to the existing solutions operating at these frequency ranges, the antenna is small-sized and low-profile due to the use of planar antenna elements and integration with a p-i-n diode-based SPDT switch.

II. ANTENNA DESIGN

The proposed antenna consists of two radiators pointing different directions that are fed by a single RF port through an SPDT switch. The radiation pattern can be reconfigured by changing the state of the switch. LTSA are used as the radiating elements due to their end-fire radiation pattern in the dielectric plane and the ease of integration with the p-i-n-diode-based distributed SPDT switch [19]. The antenna was designed on a ROGERS CuClad 217 substrate having the dielectric constant of 2.20, the thickness H of 0.254 mm, metalization layer thickness T of 35 μm, and the dissipation factor of 0.001. The electromagnetic simulations were carried out using Altair FEKO 2019.2 software.

The implementation of the proposed idea is shown in Fig. 1 and detailed view of the antenna layers is shown in Fig. 2. The designed structure is composed of two LTSAs with the opening angle α, the length L_a and the end width W_a which are

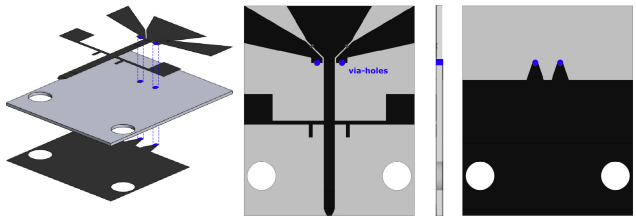

Fig. 2. Detailed view of the antenna board. (a) Exploded view. (b) Top and top, side and bottom layers view. The metalization is in black, dielectric is in gray, and via-holes are in blue.

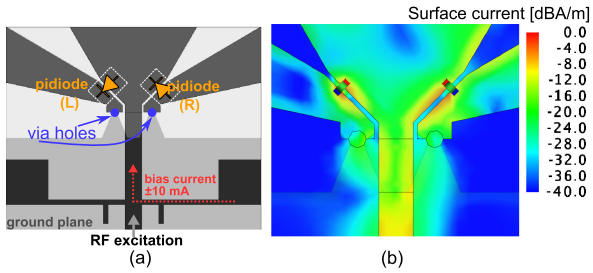

Fig. 3. Microstrip-to-dual-slotline transition. (a) Design of the transition. (b) Surface current distribution in the R configuration—the R diode is forward biased.

placed symmetrically to each other and pointing the directions $\pm\beta$ with regard to the symmetry plane of the structure. The antennas are fed through the slotlines of the width W_x which connect to the input microstrip line through a transition. This transition, shown in Fig. 3, was designed as a dual-line version of the microstrip to coplanar strips balun proposed in [20]. It consists of three strips on the top layer, two tapers on the bottom layer and two via-holes of diameter D_{via}. The tapers join the ground plane of the microstrip line with the outer strips of the slotlines through the via-holes, while the central strip expands to form the common conductor of both slotlines. The whole antenna structure is excited from a 1.0 mm end-launch connector mounted using holes of diameter $D_{\text{hole}} = 2$ mm.

The distributed SPDT switching circuit is made of two p-i-n diodes loading the slotlines in shunt configuration and placed with an offset P from the microstrip transition end. Commercially available MA4AGFCP910 p-i-n diodes are chosen due to their very low capacitance. The diodes are placed in the antiparallel configuration and biased by the common control voltage (or, equivalently, control current). When one diode is forward-biased (typically by 10 mA current flowing into the antenna circuit) the second one is reverse-biased with a negative voltage equal to the forward voltage of the first diode (typ. 1.37 V) and very small reverse leakage current (typ. 10 μA). The manufacturer provides measured two-port RF characteristics of diodes up to the frequency of 50 GHz. For the simulation purposes a one-port model is needed, so the available measurement data were converted to the required form by grounding one port of the diode. Furthermore, the diode's parameters had to be extrapolated up to 70 GHz to properly simulate the performance of the designed antenna. To this end, *RLC* equivalent circuits were derived for both forward and reverse bias states of the diode. The parameters of each model were obtained by tuning the components to fit

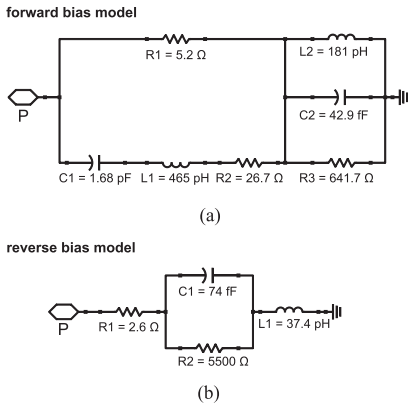

Fig. 4. Equivalent *RLC* circuits of the MA4AGFCP910 p-i-n diode as a one port model. (a) Forward bias (10 mA) diode model. (b) Reverse bias model.

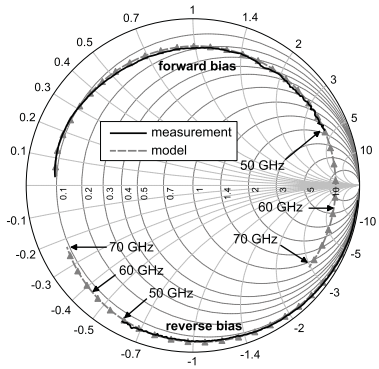

Fig. 5. Measured and modeled impedances of the MA4AGFCP910 p-i-n diodes in both forward and reverse bias state (2–70 GHz frequency range).

the simulated response of the model to the complex values of the measured parameters from the datasheet in the 2–50 GHz range. The resulting equivalent models are presented in Fig. 4. The measured and approximated *S*-parameters of the diode are compared in Fig. 5 and they show very good agreement in the whole fitting range. The extrapolated characteristics of the diode show that in the millimeter-wave range it acts quite opposite to the expected p-i-n diode behavior. In the forward state, the diode has the reflection coefficient phase close to 0° at 60 GHz which means that it behaves like an open-circuit, while in the reverse state it has the reflection coefficient phase of about −130° which is close to a short-circuit.

Due to the above presented properties of the p-i-n diodes at 60 GHz, the antenna radiates in the direction of the slotline loaded with the diode in forward state, while the radiation is suppressed in the direction of the slotline with the reverse-biased diode. This beam switching is visible in Fig. 3(b), where the surface current distribution in the *R* configuration is depicted. The state of the antenna is switched by changing the polarization of the dc current flowing into the network which changes impedances of the diodes, as summarized in Table II. The diodes' dc bias network is decoupled from the RF signal by a parallel stub with length L_{dc} placed P_{dc} away from the RF feedline (see Fig. 1) and is mirrored with regard to the center microstrip line in order to keep the symmetry of the antenna structure.

TABLE II
WORKING PRINCIPLE OF THE ANTENNA

Parameter	Value	
Bias input current	+10 mA	-10 mA
L diode bias	forward	reverse
L diode impedance at 60 GHz	open-circuit	short-circuit
R diode bias	reverse	forward
R diode impedance at 60 GHz	short-circuit	open-circuit
Antenna configuration	L	R
Direction of main lobe	$-\beta$	$+\beta$

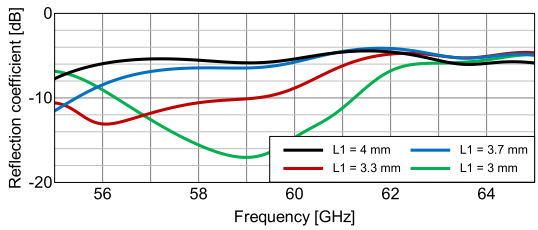

Fig. 6. Simulated input reflection coefficient of the antenna in function of length L_1. $P = 1.2$ mm.

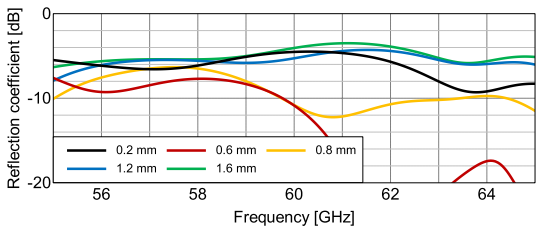

Fig. 7. Simulated input reflection coefficient of the antenna in function of diode position P. $L_1 = 4$ mm.

All the dimensions of the design (see Table I) were initially manually tuned and then optimization of the antenna's performance was conducted by a parameter sweep with the following key dimensions: L_a, W_a, L_t, W_t, P, L_1. The simulated reflection coefficient of the antenna is depicted in Figs. 6 and 7, and the simulated radiation characteristics are shown in Fig. 8. The influence of lengths L_1 and P of the radiating part of the antenna on its parameters was investigated. The impedance matching bandwidth strongly depends on these two parameters and in the best examined case covers the range of 56–61 GHz or above 60 GHz. The peak main lobe gain is approximately 2–4 dBi, depending on L_1 or P value, with about 80° half-power beamwidth. The sidelobe level decreases with increasing the L_1 length but at a cost of moving the matching bandwidth to lower frequencies. Similar effect occurs with changing the distance P. It can be seen that it is difficult to simultaneously provide good matching at 60 GHz and low sidelobes. Ultimately $L_1 = 4$ mm and $P = 1.2$ mm are chosen. Both switched beams (*L* and *R* configurations) present identical shapes but are mirrored relative to each other thus pointing two different directions as shown in in Fig. 8(d). The simulated efficiency is about 80% and the cross-polarization level in the main lobe direction is less than −10 dB.

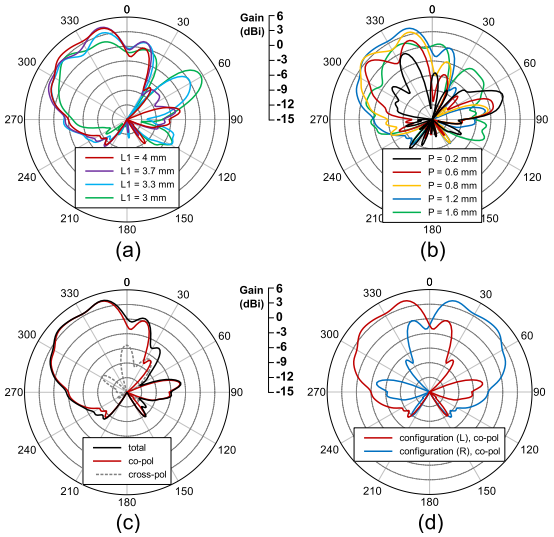

Fig. 8. Simulated radiation patterns (dBi) in the horizontal plane ($\theta = 90°$). (a) For different L_1 (L configuration only, $P = 1.2$ mm). (b) For different P ($L_1 = 4$ mm). (c) With the comparison of polarization components. (d) With the comparison of both patterns in the L and R configurations (copolarized component).

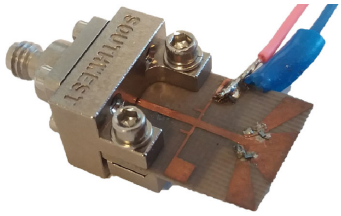

Fig. 9. Photograph of the manufactured antenna with soldered dc bias wires to control switching state of the antenna. The unused solder pad is left to maintain symmetry of the structure.

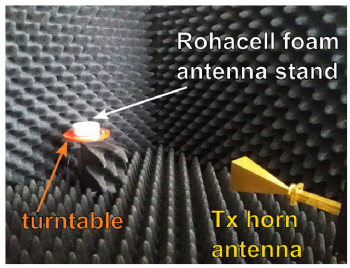

Fig. 10. Measurement setup in a millimeter-wave anechoic chamber.

III. Fabrication and Measurements

The designed antenna was fabricated in a low-cost PCB technology and the p-i-n diodes were mounted using electrically conductive silver epoxy. The manufactured antenna is shown in Fig. 9. Two wires were soldered to control the switching configuration of the antenna. A millimeter-wave anechoic chamber was constructed to conduct measurements of radiation characteristics. The measurement setup is shown in Fig. 10 and consists of an anechoic chamber and a transmitter-receiver system utilizing Rohde and Schwarz ZVA50 vector network analyzer and VDI WR15 mm-wave frequency range extension

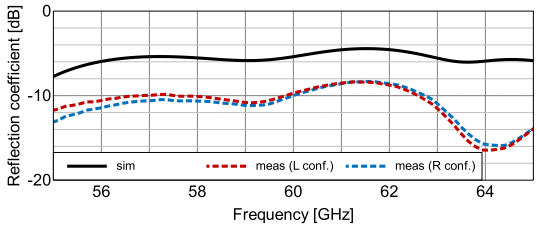

Fig. 11. Comparison of the simulated (*sim*) and measured (*meas*) input reflection coefficient characteristics of the manufactured antenna.

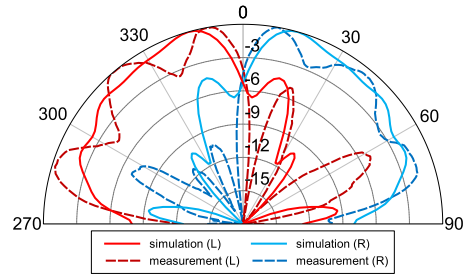

Fig. 12. Comparison of simulated and measured normalized radiation patterns (dB) in the horizontal plane ($\theta = 90°$) for both switching states at the frequency equal to 60 GHz.

modules. The antenna under test is measured in the receiving mode and is mounted on a stand made of Rohacell foam (with relative permittivity close to 1) which is placed on a turntable. This setup allows for measurements of the radiation patterns in a horizontal plane ($\theta = 90°$) in φ range of $-120°$ to $120°$ with $1°$ angular resolution.

The measured values of the reflection coefficient are shown in Fig. 11 and compared with the simulation results. There are some discrepancies that are caused by manufacturing inaccuracies and the fact that the impedances of the diodes were extrapolated. In spite of this, the antenna exhibits a satisfactory level of the reflection coefficient, which is lower than -8 dB in the whole considered band (55–65 GHz). The measured radiation patterns in the horizontal plane (see Fig. 12) show good agreement with the simulations. As initially designed, the antenna radiates in the direction of the forward-biased diode. The measured radiation patterns show a gain ripple level of about 3 dB, half-power beamwidth of about $80°$ and sidelobes at $\varphi = \pm 65°$.

IV. Conclusion

This letter presents the design and associated experimental verification of a novel simple switched-beam antenna based on a distributed SPDT switch using microstrip-to-slotline transition and p-i-n diodes, which were integrated with linear tapered slot radiators. The main beam of the antenna can be switched between two different directions. The antenna is inexpensive to manufacture and small-sized so it can be used in simple 5G network nodes, especially those that will work in Internet-of-Things systems. During the design process, we demonstrated how the commercially available p-i-n diodes characterized up to only 50 GHz can successfully be utilized in a switched-beam antenna operating in 55–65 GHz frequency range.

REFERENCES

[1] T. S. Rappaport *et al.*, "Millimeter wave mobile communications for 5G cellular: It will work!," *IEEE Access*, vol. 1, pp. 335–349, 2013.

[2] J. G. Andrews, *et al.*, "What will 5G be?" *IEEE J. Sel. Areas Commun.*, vol. 32, no. 6, pp. 1065–1082, Jun. 2014.

[3] T. Yilmaz, E. Fadel, and O. B. Akan, "Employing 60 GHz ISM band for 5G wireless communications," in *Proc. IEEE Int. Black Sea Conf. Commun. Netw.*, 2014, pp. 77–82.

[4] W. Chen *et al.*, "Ultra-low sidelobe and high gain millimeter wave microstrip array antenna," in *Proc. 6th Asia-Pacific Conf. Antennas Propag.*, 2017, pp. 1–3.

[5] I. Uchendu and J. R. Kelly, "Survey of beam steering techniques available for millimeter wave applications," *Prog. Electromagn. Res. B*, vol. 68, pp. 35–54, Mar. 2016.

[6] B. Yang, Z. Yu, J. Lan, R. Zhang, J. Zhou, and W. Hong, "Digital beamforming-based massive MIMO transceiver for 5G millimeter-wave communications," *IEEE Trans. Microw. Theory Techn.*, vol. 66, no. 7, pp. 3403–3418, Jul. 2018.

[7] L. Catarinucci, S. Guglielmi, R. Colella, and L. Tarricone, "Compact switched-beam antennas enabling novel power-efficient wireless sensor networks," *IEEE Sensors. J.*, vol. 14, no. 9, pp. 3252–3259, Sep. 2014.

[8] M. Tarkowski, M. Rzymowski, L. Kulas, and K. Nyka, "Improved jamming resistance using electronically steerable parasitic antenna radiator," in *Proc. 17th Int. Conf. Smart Technol.*, Jul. 2017, pp. 496–500.

[9] E. D. Skiani, S. A. Mitilineos, and S. C. A. Thomopoulos, "A study of the performance of wireless sensor networks operating with smart antennas," *IEEE Antennas Propag. Mag.*, vol. 54, no. 3, pp. 50–67, Jun. 2012.

[10] L. Brás, N. B. Carvalho, P. Pinho, L. Kulas, and K. Nyka, "A review of antennas for indoor positioning systems," *Int. J. Antennas Propag.*, vol. 2012, 2012, Art. no. 953269.

[11] M. Caillet, O. Lafond, and M. Himdi, "Reconfigurable microstrip antennas in millimeter waves," in *Proc. IEEE MTT-S Int. Microw. Symp. Dig.*, San Francisco, CA, USA, 2006, pp. 638–641.

[12] C. E. Patterson, W. T. Khan, G. E. Ponchak, G. S. May, and J. Papapolymerou, "A 60-GHz active receiving switched-beam antenna array with integrated Butler matrix and GaAs amplifiers," *IEEE Trans. Microw. Theory Techn.*, vol. 60, no. 11, pp. 3599–3607, Nov. 2012.

[13] S. Lee *et al.*, "A V-band beam-steering antenna on a thin-film substrate with a flip-chip interconnection," in *IEEE Microw. Wireless Compon. Lett.*, vol. 18, no. 4, pp. 287–289, Apr. 2008.

[14] A. Artemenko, A. Maltsev, A. Mozharovskiy, A. Sevastyanov, V. Ssorin, and R. Maslennikov, "Millimeter-wave electronically steerable integrated lens antennas for WLAN/WPAN applications," *IEEE Trans. Antennas Propag.*, vol. 61, no. 4, pp. 1665–1671, Apr. 2013.

[15] A. Moknache *et al.*, "A switched-beam linearly-polarized transmitarray antenna for V-band backhaul applications," in *Proc. 10th Eur. Conf. Antennas Propag.*, 2016, pp. 1–5.

[16] V. Semkin *et al.*, "Beam switching conformal antenna array for mm-wave communications," *IEEE Antennas Wireless Propag. Lett.*, vol. 15, pp. 28–31, 2016.

[17] M. Rzymowski, K. Trzebiatowski, K. Nyka, and L. Kulas, "DoA estimation using reconfigurable antennas in millimeter-wave frequency 5G systems," in *Proc. 17th IEEE Int. NEWCAS Conf.*, Munich, Germany, 2019, pp. 1–4.

[18] S. Cheng *et al.*, "Switched beam antenna based on RF MEMS SPDT switch on quartz substrate," *IEEE Antennas Wireless Propag. Lett.*, vol. 8, pp. 383–386, 2009.

[19] Z. Lu, X. Yang, and G. Tan, "A wideband printed tapered-slot antenna with pattern reconfigurability," *IEEE Antennas Wireless Propag. Lett.*, vol. 13, pp. 1613–1616, 2014.

[20] Z. C. Zheng and G. Q. Luo, "Design of a compact wideband balun between microstrip and coplanar stripline," in *Proc. IEEE MTT-S Microw. Workshop Ser. Millim. Wave Wireless Technol. Appl.*, 2012, pp. 1–3.